The Journal of Infectious Diseases

BRIEF REPORT

A Role for Taok2 in *Listeria monocytogenes* Vacuolar Escape

Juan J. Quereda,[1,2] Camille Morel,[1] Noelia Lopez-Montero,[3,4] Jason Ziveri,[5,6] Steven Rolland,[1] Théodore Grenier,[7] Nathalie Aulner,[8] Anne Danckaert,[8] Alain Charbit,[5,6] Jost Enninga,[3,4] Pascale Cossart,[1] and Javier Pizarro-Cerdá[9]

[1] Unité des Interactions Bactéries-Cellules, Institut Pasteur, Paris, France, [2]Departamento Producción y Sanidad Animal, Salud Pública Veterinaria y Ciencia y Tecnología de los Alimentos. Facultad de Veterinaria. Universidad Cardenal Herrera-CEU, CEU Universities. Valencia, Spain, [3]Unité Dynamique des Interactions Hôte-Pathogène, Institut Pasteur, Paris, France, [4]Institut Pasteur, CNRS UMR3691, Paris, France, [5]Université Paris Descartes, Sorbonne Paris Cité, Paris, France, [6]Institut Necker-Enfants Malades, INSERM U1151-CNRS UMR 8253, Paris, France, [7]Institut de Génomique Fonctionnelle de Lyon, Université de Lyon, Ecole Normale Supérieure de Lyon, CNRS UMR 5242, Lyon, France, [8]Unité de Technologie et de Services Photonic BioImaging/Centre de Ressources et de Recherches Technologiques, Institut Pasteur, Paris, France, and [9]Unité de Recherche Yersinia, Institut Pasteur, Paris, France

The bacterial pathogen *Listeria monocytogenes* invades host cells, ruptures the internalization vacuole, and reaches the cytosol for replication. A high-content small interfering RNA (siRNA) microscopy screen allowed us to identify epithelial cell factors involved in *L. monocytogenes* vacuolar rupture, including the serine/threonine kinase Taok2. Kinase activity inhibition using a specific drug validated a role for Taok2 in favoring *L. monocytogenes* cytoplasmic access. Furthermore, we showed that Taok2 recruitment to *L. monocytogenes* vacuoles requires the presence of pore-forming toxin listeriolysin O. Overall, our study identified the first set of host factors modulating *L. monocytogenes* vacuolar rupture and cytoplasmic access in epithelial cells.

Keywords. *Listeria monocytogenes*; Taok2; STE1-like kinase; vacuolar escape; siRNA screen.

The gram-positive pathogen *Listeria monocytogenes* is a major model microorganism to understand bacterial subversion of host functions in the context of disease. *L. monocytogenes* is a facultative intracellular pathogen able to invade mammalian cells. Upon interaction of bacterial surface molecules (InlA, InlB) with host receptors (E-cadherin, Met), signaling cascades are triggered to promote actin rearrangements and bacterial engulfment. Rupture of the internalization vacuole allows *L. monocytogenes* to reach the cytosol, where it replicates [1].

Received 18 April 2020; editorial decision 16 June 2020; accepted 19 June 2020; published online June 25, 2020.

Correspondence: Dr J. Pizarro-Cerdá, Unité de Recherche Yersinia, 28, rue du Docteur Roux, Institut Pasteur, 75724, Paris, France (javier.pizarro-cerda@pasteur.fr).

The Journal of Infectious Diseases® 2022;225:1005–10

DOI: 10.1093/infdis/jiaa367

Three *L. monocytogenes* exotoxins control vacuolar escape: a phosphatidylinositol-specific phospholipase C (PlcA), a broad-range phospholipase C (PlcB), and the cholesterol-dependent cytotoxin listeriolysin O (LLO) [1]. In phagocytic cells, host factors have also been recognized as modulators of *L. monocytogenes* vacuolar rupture, including γ-interferon–inducible lysosomal thiol reductase (GILT), cystic fibrosis transmembrane conductance regulator (CFTR), and calpain [2]. Whether host factors in nonphagocytic cells control *L. monocytogenes* vacuolar escape has not been explored so far.

In the present study, we used a high-content microscopy approach to identify epithelial host cell components specifically required for efficient rupture of the *L. monocytogenes*-containing vacuole.

METHODS

Bacterial and Mammalian Growth Conditions, Plasmids, Drugs, and Infections

Bacterial strains were: *L. monocytogenes* EGDe PrfA* (BUG 3057), EGDe PrfA*$^{\beta\text{-lact}}$ (BUG 3358), EGDe PrfA* Δ*plcA*Δ*plcB* (BUG3620), EGDe PrfA* Δ*hly*Δ*plcA*Δ*plcB* (BUG 3648), *L. innocua*$^{\beta\text{-lact/InlB}}$ (BUG 3614) [3], *Shigella flexneri* wild-type strain M90T expressing the adhesin AfaI [4], *Francisella tularensis* subsp. *novicida* strain U112 (or *F. novicida* wild type), and an isogenic strain with the *Francisella* pathogenicity island (Δ*FPI*) deleted [5]. The plasmid encoding YFP-CBD, a yellow fluorescent protein (YFP) chimera protein of the cell wall binding domain (CBD) from the *Listeria* phage endolysin Ply118, has been described [6]. The plasmids encoding actin-mOrange and galectin-3-enhanced green fluorescent protein (EGFP) were used as a markers for ruffle formation and vacuole lysis by *S. flexneri* [4]. Human HeLa cells (American Type Culture Collection CCL-2) were transfected with 1.5 μg of the plasmids encoding YFP-CBD, actin-mOrange, or galectin-3-EGFP using Lipofectamine LTX for 24 hours. Bacterial strains and Hela cells were grown as described [3]. The specific Taok2 inhibitor SW172006 (Chembridge) [7] was added to HeLa cells at 50 μM for 24 hours before infection.

L. monocytogenes infections were performed as described [8, 9] to: (1) assess the efficiency of *L. monocytogenes* EGDe PrfA* invasion into HeLa cells treated with dimethyl sulfoxide (DMSO) or SW172006 at 1 hour post infection (hpi); (2) identify cytosolic bacteria labeled with CBD following vacuolar escape after Taok2 knockdown using small interfering RNA (siRNA) or after Taok2 kinase activity inhibition using SW172006 at 1 hpi (100 cells were counted in 3 representative fields to estimate the number of CBD-labeled bacteria); (3) perform immunofluorescence studies to analyze

the distribution of Taok2 in HeLa cells at 30 minutes post infection (mpi); and (4) quantify the number of intracellular bacteria that escape from vacuoles and are associated with actin at 5 hpi after Taok2 siRNA knockdown. The multiplicity of infection (MOI) used was 25 (EGDe PrfA*), 50 (EGDe PrfA* Δ*plcA*Δ*plcB*), or 125 (EGDe PrfA* Δ*hly*Δ*plcA*Δ*plcB*). *S. flexneri* infections were performed as described [4]. HeLa cells transfected with scrambled or Taok2 siRNAs were infected (37°C, MOI 50), and live imaging of *S. flexneri* vacuolar rupture was monitored and quantified as the time interval between ruffle formation and appearance of a galectin-3 signal around the bacteria. Images were recorded in a Nikon Ti-E microscope (× 20 objective) with a time lapse of 2 minutes for 2 hours. *F. novicida* infections were performed using a MOI of 1000. Bacterial entry synchronization was performed by a 5-minute centrifugation at 1000 rpm and plates incubated at 37°C. After 1 hour plates were incubated at 37°C in fresh medium supplemented with gentamycin for 24 hours. Bacterial multiplication was monitored by plating cell lysates on chocolate agar plates. Each experiment was conducted at least twice in triplicates.

siRNA Library Screen

Four distinct oligos were used for each target gene. The screen was performed as described [4]. Each 96-well screen plate contained: 8 positive control wells transfected with scrambled siRNA and challenged with *L. monocytogenes* EGDe PrfA*$^{\beta\text{-lact}}$ [3]; 8 negative control wells transfected with scrambled siRNA and challenged with invasive *L. innocua*$^{\beta\text{-lact/InlB}}$ (which invades host cells but remains trapped in vacuoles); and 4 replicates for each siRNA target infected with *L. monocytogenes* EGDe PrfA*$^{\beta\text{-lact}}$. Reverse siRNA transfection of HeLa cells was performed using Lipofectamine RNAi Max at a 10-nM siRNA concentration for 72 hours. The CCF4 assay for *L. monocytogenes* vacuole rupture quantification and differential staining of extracellular versus total *L. monocytogenes* for cell entry quantification at 1 hpi was performed as described [3, 7]. Images were acquired on a confocal microscope Opera QEHS (PerkinElmer) as described [3, 7]. The strictly standardized mean difference (SSMD) statistical test was used for quality control analysis and for hit scoring [3, 7].

Image Acquisition

Bacterial cytoplasmic access was determined by actin comet tail formation using phalloidin [9]. Briefly, extracellular *L. monocytogenes* were labeled with a primary goat anti-*L. monocytogenes* serum and with a secondary chicken anti-goat Alexa 647. Cells were permeabilized using 0.1% Triton X-100 and total *L. monocytogenes* were labeled with the same primary antibody and a secondary chicken anti-goat Alexa 488. Actin was labeled with phalloidin Alexa 546. At 5 hpi, cytosolic bacteria were those stained with Alexa 546 and Alexa 488 but lacking Alexa 647. In 3 representative fields 100 cells were counted to estimate the number of cytosolic *L. monocytogenes* cells.

For Taok2 labeling, 96-well tissue culture plates were seeded with HeLa cells to reach 80% confluence on the infection day. Cell infection with indicated strains was performed as reported [9]. At 1 hpi cells were washed and fixed with a paraformaldehyde (4% in phosphate-buffered saline) for 15 minutes. Extracellular *L. monocytogenes* were labeled with a primary rabbit anti-*L. monocytogenes* serum and with a secondary goat anti-rabbit Alexa 647. Next, cells were permeabilized using 0.1% Triton X-100 for 4 minutes. Taok2 was labeled overnight at 4°C with a mouse monoclonal antibody (Santa Cruz 514268) and a secondary goat anti-mouse Alexa 488. Actin was labeled with phalloidin Alexa 546. DNA was stained with Hoechst 33342.

Statistical Analysis

Statistical analysis was performed with GraphPad Prism v6. Differences between control and experimental groups were evaluated by 2-tailed unpaired *t* tests or 1-way ANOVA followed by a Dunnett multiple comparison test. $P < .05$ was considered as significant.

RESULTS

Identification of Host Factors Controlling *L. monocytogenes* Vacuolar Escape in Epithelial Cells

To identify epithelial host cell factors specifically involved in *L. monocytogenes* vacuolar escape, we exploited a previous genome-wide siRNA screen that distinguished host genes modulating the cytoplasmic accumulation of the *L. monocytogenes* secreted molecule InlC (an event requiring *L. monocytogenes* cell invasion, vacuolar escape, and cytoplasmic proliferation) [10]. We siRNA-inactivated the 165 most significant hits identified in this previous screen and performed a novel high-content microscopy screen in which we combined: (1) a CCF4 fluorescence resonance energy transfer (FRET)-based assay to measure *L. monocytogenes* vacuolar rupture and cytoplasmic access [3, 7], and (2) a differential immunofluorescence staining to distinguish extracellular versus total *L. monocytogenes* [3, 7].

Fifty siRNA targeted genes were identified as extremely strong hits affecting *L. monocytogenes* vacuolar escape (Figure 1A–C and Supplementary Table 1). Some of these genes displayed either inhibition of bacterial entry into host cells (*PODXL*, *SLC12A4*, *USE1*, and *TTC19*) or induced strong cytotoxicity (*PPP3R2*) (Supplementary Table 1). However, we also identified genes that had a bona fide effect on *L. monocytogenes* cytoplasmic access and did not affect bacterial entry or cell integrity (*EED*, *KAT5*, *MTOR*, *SYK*, *TAOK2*, *DPEP1*, and *PIGL*) (Figure 1A–C and Supplementary Table 1).

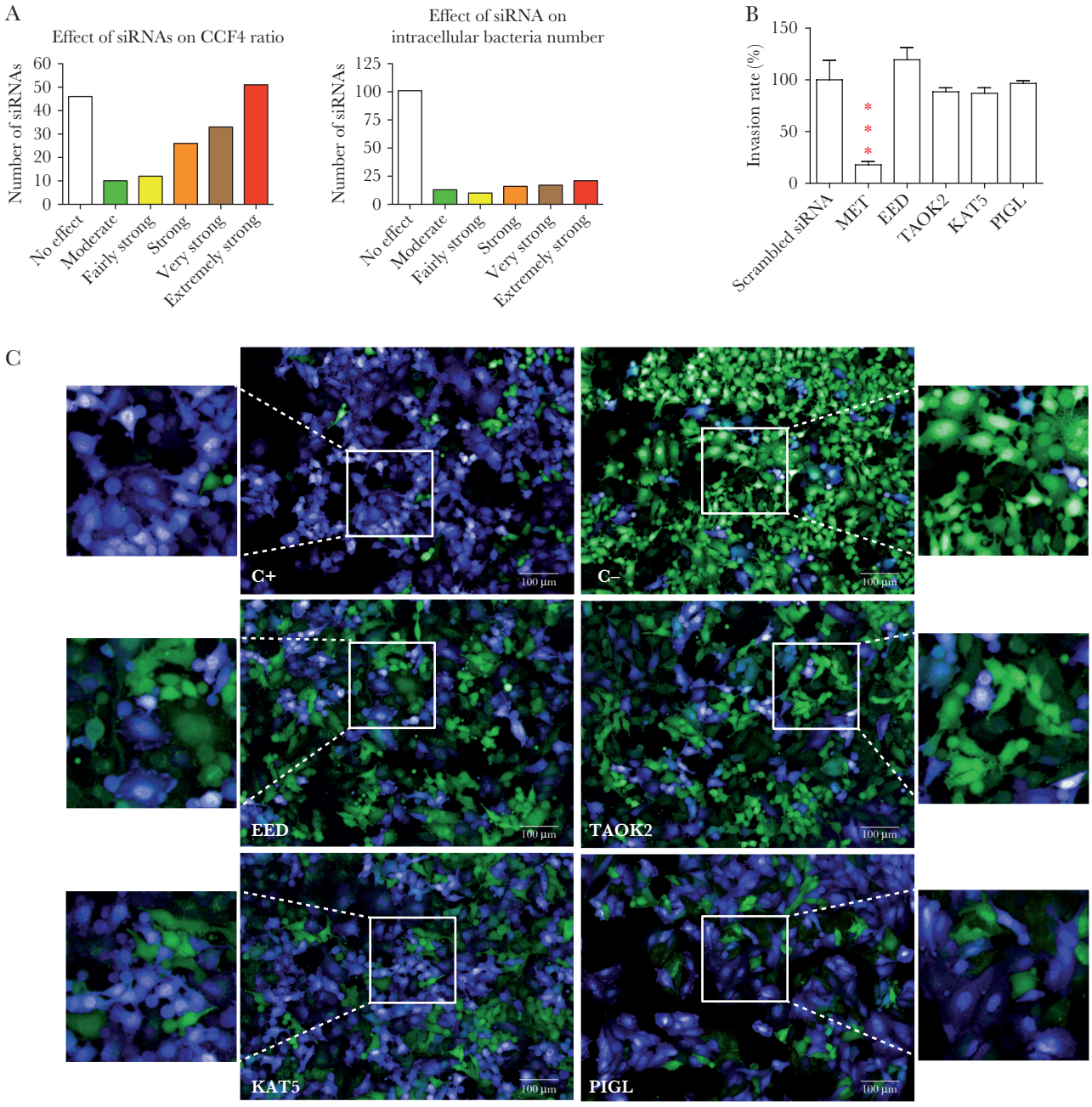

Figure 1. High-content microscopy siRNA screen reveals host factors required by *Listeria monocytogenes* for vacuolar escape in epithelial cells. *A*, Overview of the screen results. After data normalization based on the strictly standardized mean difference method, 165 targeted genes were classified into 6 categories based on their effect on the FRET probe CCF4 green to blue ratio (vacuolar escape step, left) and in the intracellular bacteria number (entry step, right): no effect, moderate, fairly strong, strong, very strong, and extremely strong effects. *B*, Contributions of *MET* (control for invasion), *EED*, *TAOK2*, *KAT5*, and *PIGL* to *L. monocytogenes* invasion. Target genes were knocked down by siRNA transfection of HeLa cells. One hour after infection cells were washed and *L. monocytogenes* entry was measured by counting colony forming units. Bars represent the mean and SD from 3 experiments. Significant differences from the scramble treatment *** $P < .001$. *C*, Examples of images from the siRNA screen. HeLa cells were grown in 96-well plates and transfected by siRNAs. Host cells were loaded with CCF4-AM and infected with *L. monocytogenes* EGDe PrfA*$^{\beta\text{-lact}}$ (C+) or *L. innocua*$^{\beta\text{-lact/InlB}}$ (C–) for 1 hour. C+ and C– negative wells were transfected with scrambled siRNA. After paraformaldehyde fixation, nuclei were stained with Draq5 and cells were imaged using an Opera QEHS confocal microscope, as previously described [3]. Images were obtained with the following merged channels: the intact CCF4 probe peaks at 535 nm (green), and the cleaved CCF4 probe peaks at 450 nm (blue). *L. monocytogenes* EGDe PrfA*$^{\beta\text{-lact}}$ (C+) can escape its vacuolar compartments and induce the cleavage of the CCF4 probe (top left). Scale bar 100µm. Abbreviations: FRET, fluorescence resonance energy transfer; siRNA, small interfering RNA.

Taok2 Controls *L. monocytogenes* Vacuolar Escape

We selected Taok2 for further validation based on its strong phenotype and on reports showing its localization to vesicular compartments and its implication in surface receptor endocytosis [11, 12]. Taok2 depletion efficiency was verified by quantitative reverse transcription polymerase chain reaction

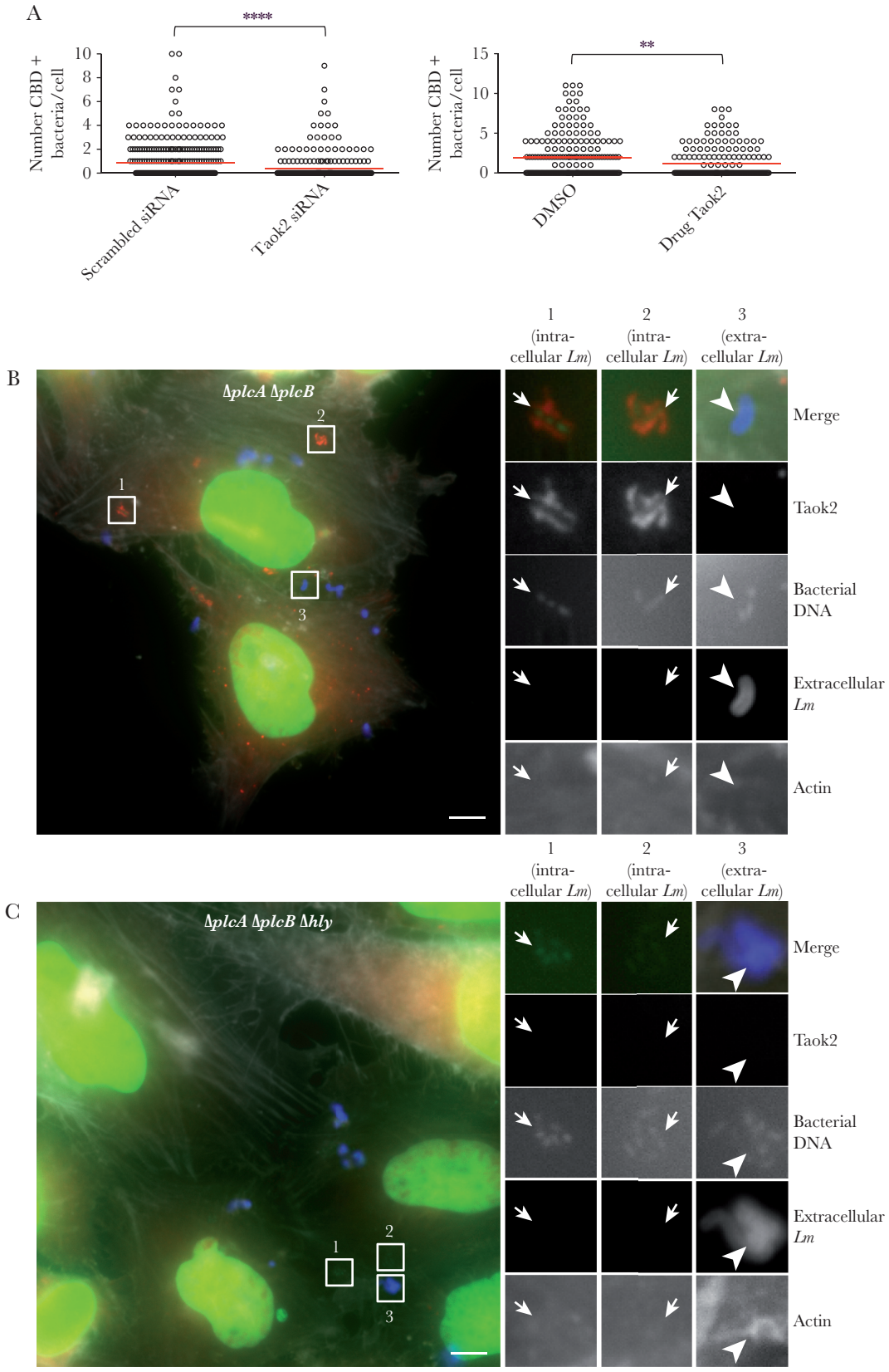

Figure 2. Taok2 siRNA knockdown or inhibition of its kinase activity by the chemical compound SW172006 impairs efficient rupture of *Listeria monocytogenes*-containing vacuoles. *A*, Taok2 knockdown by siRNA (left) or inhibition of its kinase activity (right) results in reduced cytoplasmic access. HeLa cells were transfected with the YFP-CBD of the *L. monocytogenes* phage endolysin Ply118, which identifies cytosolic bacteria shortly after escape. The red line indicates the mean. Results were from 100 cells counted in 3 representative fields to estimate the number of CBD-labeled bacteria. Statistical analysis: 2-tailed unpaired *t* tests. $^{**}P < .01$, $^{****}P < .0001$. *B* and *C*, Taok2 accumulation

(qRT-PCR; Supplementary Figure 1A). We investigated the impact of Taok2 depletion on *L. monocytogenes* cytoplasmic access using as readout the recruitment of the fluorescent chimera of the cell wall-binding domain (YFP-CBD) of the *L. monocytogenes* phage endolysin Ply118 [6], which labels cytosolic bacteria shortly after vacuolar escape [6]. After 1 hpi, Taok2 knockdown significantly reduced the number of YFP-CBD–positive *L. monocytogenes* per infected HeLa cell, in comparison to cells treated with control siRNA (0.90 for scrambled siRNA vs 0.36 for Taok2 siRNA; $P < .0001$; Figure 2A).

We next used a small molecule (SW172006) that specifically inhibits the kinase activity of Taok2 [13]. We demonstrated by gentamicin assays that *L. monocytogenes* entry is not affected in cells treated with SW172006 (Supplementary Figure 1B). Importantly, Taok2 kinase activity inhibition caused a decrease in the number of YFP-CBD–positive *L. monocytogenes* per infected HeLa cell (1.99 for DMSO vs 1.27 for Taok2 SW172006; $P < .01$; Figure 2A), confirming our previous siRNA results (Figure 1). We then quantified in Taok2-depleted cells the number of cytoplasmic *L. monocytogenes* decorated with actin at 5 hpi. Taok2 depletion significantly increased the percentage of actin-negative (vacuole-trapped) *L. monocytogenes* in comparison to cells treated with control siRNA (13.5% for scrambled siRNA vs 38.5% for Taok2 siRNA; $P < .05$; Supplementary Figure 1C). Altogether, these results demonstrate that Taok2 enhances *L. monocytogenes* vacuolar rupture in HeLa cells.

Taok2 Is Recruited to *L. monocytogenes* Vacuoles

We next analyzed the distribution of Taok2 in *L. monocytogenes*-infected HeLa cells. Using anti-Taok2 antibodies, we observed rare events of Taok2 association with the *L. monocytogenes* EGDe PrfA* strain (not shown), suggesting that Taok2 recruitment to *L. monocytogenes* vacuoles is transient. We hypothesized that by delaying *L. monocytogenes* vacuolar escape, we might increase the probability of detecting Taok2 recruitment. Indeed, when using an *L. monocytogenes* EGDe PrfA*Δ*plcA*Δ*plcB* strain, which lacks both phospolipases C and displays delayed vacuolar escape [14], we were able to observe a clearer association of Taok2 with *L. monocytogenes* in a compartment resembling a bacteria-containing vacuole (Figure 2B). Taok2 recruitment was abolished when using an EGDe PrfA*Δ*plcA*Δ*plcB*Δ*hly* strain lacking the phospholipases and LLO, demonstrating that Taok2 recruitment is dependent on LLO production (Figure 2C).

Taok2 Does Not Affect *S. flexneri* or *F. novicida* Cytoplasmic Translocation

We evaluated whether Taok2 displays a general role on vacuolar rupture for bacterial pathogens other than *L. monocytogenes* by analyzing its contribution to the cytoplasmic access of *S. flexneri* and *F. novicida,* 2 gram-negative pathogens that rupture their internalization vacuole as *L. monocytogenes*. Using a galectin-3 readout that follows the same principle of the YFP-CBD readout described above, we did not observe any role for Taok2 in *S. flexneri* cytoplasmic access (Supplementary Figure 1D). Furthermore, using gentamicin assays we did not detect any contribution of Taok2 to the late replication (24 hpi) of *F. novicida* (Supplementary Figure 1E), indirectly suggesting that Taok2 does not affect its cytoplasmic translocation.

DISCUSSION

Our results identify Taok2 as the first host cell factor specifically affecting vacuolar rupture and cytoplasmic translocation of *L. monocytogenes* in epithelial cells. Taok2 is a poorly studied serine/threonine kinase that belongs to the MAP3K family, which has been associated with neurological disorders [11, 15]. Taok2 has been localized to vesicular compartments, has been implicated in the endocytosis of N-cadherin at the synapse, and phosphorylates members of the septin family in neurons [11, 12, 15]. Our results therefore suggest a broader role for Taok2 in controlling integrity of phagosomal vacuoles. As our microscopy study highlights that Taok2 can be directly recruited by intracellular *L. monocytogenes,* and the use of the SW172006 inhibitor indicates that the Taok2 kinase activity is required for its role in *L. monocytogenes* vacuolar escape, our hypothesis is that Taok2 phosphorylates an unknown factor that is probably also recruited to the *L. monocytogenes* vacuole and which plays a more direct role on facilitating vacuolar rupture. Our results indicating that Taok2 association with *L. monocytogenes* vacuoles is dependent on LLO production suggest either that specific membrane damages produced by LLO are the signal triggering Taok2 vacuolar recruitment or, alternatively, that Taok2 recruitment is driven by other *L. monocytogenes* components being exposed to the cytosolic environment upon effective vacuolar rupture mediated by LLO. The molecular cascade of events downstream of Taok2 that leads to facilitated *L. monocytogenes* vacuolar rupture remains to be identified.

Apart from Taok2, we also found other host genes with a strong effect on *L. monocytogenes* vacuolar rupture and no effect on entry. These results propose a multifaceted mechanism

in a compartment resembling a *L. monocytogenes*-containing vacuole. *B*, HeLa cells infected with *L. monocytogenes* EGDe PrfA*Δ*plcA*Δ*plcB* for 30 minutes and imaged. Taok2 (labeled with anti-Taok2 antibodies) is shown in red, DNA (labeled with Hoechst) is shown in green, extracellular bacteria (labeled with anti-*L. monocytogenes* antibodies) are shown in blue, and actin (labeled with phalloidin) is shown in white. Left image: overview. Right images: enlargement of 3 ROIs shown in the overview. In ROIs 1 and 2, Taok2 decorates intracellular bacteria (small arrows, revealed by the bacterial DNA labeling and by the absence of extracellular bacterial labeling), which are present in a vacuolar compartment and do not polymerize cytoplasmic actin (absence of actin labeling). In ROI 3, extracellular bacteria (large arrowhead, revealed by the presence of both DNA and extracellular *L. monocytogenes* labeling) are not decorated by Taok2. Scale bar, 5 µm. *C*, HeLa cells infected as in (*B*) using the strain *L. monocytogenes* EGDe PrfA* Δ*plcAΔplcBΔhly*. Left image: overview. Right images: enlargement of 3 ROIs shown in the overview. In all the ROIs showing either intracellular or extracellular *L. monocytogenes* Taok2 does not decorate the bacteria. Scale bar, 5 µm. Abbreviations: CBD, cell wall binding domain; DMSO, dimethyl sulfoxide; LM, *Listeria monocytogenes*; ROI, regions of interest; siRNA, small interfering RNA; YFP, yellow fluorescent protein.

where several host pathways are hijacked by *L. monocytogenes* to control vacuolar rupture.

Supplementary Data

Supplementary materials are available at *The Journal of Infectious Diseases* online. Consisting of data provided by the authors to benefit the reader, the posted materials are not copyedited and are the sole responsibility of the authors, so questions or comments should be addressed to the corresponding author.

Notes

Financial support. This work was supported by *Institut Pasteur, Université Paris Diderot, Agence Nationale de la Recherche* (grant numbers ANR-15-CE15-0017 StopBugEntry to J. P. C., J. E., and A. C.; and ANR-10-INSB-04-01, France-BioImaging to N. A.). J. J. Q. is supported by *the Spanish Ministry of Science, Innovation and Universities* (grant number RYC-2018-024985-I *Ramón y Cajal contract*). J. E. was supported by the European Research Council (consolidator grant EndoSubvert). P. B. I. is supported by the *Région Ile de France* (DIM1Health) and Groupement d'Intérêt Scientifique Infrastructures en Biologie Santé et Agronomie. The teams of P. C., J. P. C., N. A., and J. E. are members of Laboratory of Excellence Integrative Biology of Emerging Infectious Diseases.

Potential conflicts of interest. All authors: No reported conflicts of interest. All authors have submitted the ICMJE Form for Disclosure of Potential Conflicts of Interest. Conflicts that the editors consider relevant to the content of the manuscript have been disclosed.

References

1. Pizarro-Cerdá J, Cossart P. Microbe profile: *Listeria monocytogenes*: a paradigm among intracellular bacterial pathogens. Microbiology **2019**; 165:719–21.
2. Pizarro-Cerda J, Cossart P. *Listeria monocytogenes*: cell biology of invasion and intracellular growth. Microbiol Spectr **2018**; 6:10.1128/microbiolspec.GPP3-0013-2018.
3. Quereda JJ, Pizarro-Cerdá J, Balestrino D, et al. A dual microscopy-based assay to assess *Listeria monocytogenes* cellular entry and vacuolar escape. Appl Environ Microbiol **2016**; 82:211–7.
4. Mellouk N, Weiner A, Aulner N, et al. *Shigella* subverts the host recycling compartment to rupture its vacuole. Cell Host Microbe **2014**; 16:517–30.
5. Weiss DS, Brotcke A, Henry T, Margolis JJ, Chan K, Monack DM. In vivo negative selection screen identifies genes required for *Francisella* virulence. Proc Natl Acad Sci U S A **2007**; 104:6037–42.
6. Henry R, Shaughnessy L, Loessner MJ, Alberti-Segui C, Higgins DE, Swanson JA. Cytolysin-dependent delay of vacuole maturation in macrophages infected with *Listeria monocytogenes*. Cell Microbiol **2006**; 8:107–19.
7. Quereda JJ, Sachse M, Balestrino D, et al. Assessing vacuolar escape of *Listeria monocytogenes*. Methods Mol Biol **2017**; 1535:173–95.
8. Mostowy S, Danckaert A, Tham TN, et al. Septin 11 restricts InlB-mediated invasion by *Listeria*. J Biol Chem **2009**; 284:11613–21.
9. Quereda JJ, Nahori MA, Meza-Torres J, et al. Listeriolysin S is a streptolysin S-like virulence factor that targets exclusively prokaryotic cells in vivo. MBio **2017**; 8:e00259-17.
10. Kühbacher A, Emmenlauer M, Rämo P, et al. Genome-wide siRNA screen identifies complementary signaling pathways involved in *Listeria* infection and reveals different actin nucleation mechanisms during *Listeria* cell invasion and actin comet tail formation. mBio **2015**; 6:e00598-15.
11. Yasuda S, Tanaka H, Sugiura H, et al. Activity-induced protocadherin arcadlin regulates dendritic spine number by triggering N-cadherin endocytosis via TAO2beta and p38 MAP kinases. Neuron **2007**; 56:456–71.
12. Moore TM, Garg R, Johnson C, Coptcoat MJ, Ridley AJ, Morris JD. PSK, a novel STE20-like kinase derived from prostatic carcinoma that activates the c-Jun N-terminal kinase mitogen-activated protein kinase pathway and regulates actin cytoskeletal organization. J Biol Chem **2000**; 275:4311–22.
13. Piala AT, Akella R, Potts MB, et al. Discovery of novel TAOK2 inhibitor scaffolds from high-throughput screening. Bioorg Med Chem Lett **2016**; 26:3923–7.
14. Smith GA, Marquis H, Jones S, Johnston NC, Portnoy DA, Goldfine H. The two distinct phospholipases C of *Listeria monocytogenes* have overlapping roles in escape from a vacuole and cell-to-cell spread. Infect Immun **1995**; 63:4231–7.
15. Yadav S, Oses-Prieto JA, Peters CJ, et al. TAOK2 kinase mediates PSD95 stability and dendritic spine maturation through Septin7 phosphorylation. Neuron **2017**; 93:379–93.